Published in final edited form as:
J Neurosci. 2010 April 7; 30(14): 5008–5019. doi:10.1523/JNEUROSCI.6260-09.2010.

Early suppressive mechanisms and the negative BOLD response in human visual cortex

Alex R. Wade[1,2] and **Jess Rowland**[1]
Smith-Kettlewell Eye Research Institute, CA
University of California San Francisco, CA

Abstract

Functional magnetic resonance imaging (fMRI) studies of early sensory cortex often measure stimulus-driven increases in the blood oxygenation level-dependent (BOLD) signal. However, these positive responses are frequently accompanied by reductions in the BOLD signal in adjacent regions of cortex. Although this negative BOLD response (NBR) is thought to result from neuronal suppression, the precise relationship between local activity, suppression and perception remains unknown. By measuring BOLD signals in human primary visual cortex while varying the baseline contrast levels in the region affected by the NBR, we tested three physiologically-plausible computational models of neuronal modulation which could explain this phenomenon: a subtractive model, a response gain model and a contrast gain model. We also measured the ability of isoluminant contrast to generate an NBR. We show that the NBR can be modeled as a pathway-specific contrast gain modulation that is strongest outside the fovea. We found a similar spatial bias in a psychophysical study using identical stimuli, although these data indicated a response- rather than a contrast-gain mechanism. We reconcile these findings by proposing 1) that the NBR is associated with a long-range suppressive mechanism that hyperpolarizes a subset of magnocellularly-driven neurons at the input to V1; 2) that this suppression is broadly-tuned to match the spatial features of the mask region; 3) that increasing the baseline contrast in the suppressed region drives all neurons in the input layer, reducing the relative contribution of the suppressing subpopulation in the fMRI signal.

Keywords

fMRI; BOLD; surround suppression; extraclassical RF; magnocellular; parvocellular

Introduction

Researchers using functional magnetic resonance imaging (fMRI) often observe a stimulus-driven reduction in the fMRI in the blood oxygenation (BOLD) signal in response to a visual stimulus. This ‘negative BOLD response’ (NBR) occurs within retinotopic sensory cortex at some distance from the directly-stimulated region (Tootell, Mendola et al. 1998; Harel, Lee et al. 2002; Shmuel, Yacoub et al. 2002; Smith, Williams et al. 2004). The NBR is time-locked to the onset of the stimulus and has a similar timecourse to the positive BOLD response (PBR) (Shmuel, Yacoub et al. 2002; Shmuel, Augath et al. 2006). Although hemodynamic effects may explain a small part of the NBR (Harel, Lee et al. 2002; Boas, Jones et al. 2008), two observations suggest that the effect is largely driven by active neuronal mechanisms. Firstly, the NBR can be found in the opposite cerebral hemisphere to

Corresponding author: Alex R. Wade, SKERI, 2318 Fillmore St, San Francisco, CA 94115, wade@wadelab.net.

the PBR (Smith, Williams et al. 2004). Because there is no spatially-specific vascular coupling between the two halves of primate visual cortex, no hemodynamic mechanism could generate a response of this type. Secondly, and more directly, it has been shown that the NBR is temporally and spatially correlated with a decrease in membrane potential corresponding to an active suppressive mechanism (Shmuel, Augath et al. 2006; Devor, Tian et al. 2007). In primate visual cortex (Shmuel, Augath et al. 2006) this leads to a measurable reduction in the baseline neural spiking rate (Shmuel, Augath et al. 2006).

The NBR therefore appears to reflect suppression of neural activity at a population level. Here, we describe how we were able to test three standard computational models of neural suppression by measuring the size of the NBR as a function of ongoing activity in an annular subregion of the parafovea.

Our experiments contained stimuli in which the annulus itself had a high, near-saturating contrast while the central 'inducer' region was blank. We expected these conditions to generate an NBR in the foveal representation of primary visual cortex, yet none was observed. We hypothesized that this asymmetry reflected the change in the density of magnocellular cells across the visual field. We tested this by performing a final set of fMRI experiments in which the NBR was generated either by isoluminant red-green stimuli, which should generate very little activity in the magnocellular pathway, or by achromatic luminance stimuli which should generate a lot. We found that these stimuli generated equally strong responses in the fovea but very different levels of NBR in the parafovea. Isoluminant red-green inducers generated relatively little NBR, suggesting that this phenomenon is driven primarily by the magnocellular pathway.

Finally, we conducted a series of psychophysical experiments to examine the relationship between the NBR and perception. Consistent with the fMRI data (and earlier psychophysical studies) we found little evidence of perceptual suppression in the fovea but strong suppression in the parafovea.

Methods

fMRI methods

Subjects—Nine subjects (six males) with ages between 23 and 68 participated in our fMRI experiments. All subjects had normal or corrected-to-normal acuity, normal color vision and were experienced psychophysical observers. Seven of the subjects were naïve to the purpose of the experiment. Subjects were screened and consented in accordance with human subject protocols at both the University of California, San Francisco (UCSF), and the Smith-Kettlewell Eye Research Institute (SKERI).

Data collection and processing—fMRI data were collected on a Siemens 3T Tim Trio system at the UCSF Neuroscience Imaging Center using a standard Siemens EPI Gradient Echo sequence and 30 functional imaging planes with resolution of 1.7×1.7×2mm collected each TR (2s). Each run contained 184 TRs and a session consisted of at least 6 functional runs. Additional 'inplane' anatomical scans (T1-weighted 2D SPGR) were acquired with the same slice prescription as the T2* data in order to facilitate *post-hoc* alignment to a high-resolution anatomical dataset collected on a separate occasion.

Anatomical segmentation—High-resolution whole-head anatomical volumes were acquired on each subject to provide a canonical reference frame for subsequent functional datasets and to enable the restriction of functional data to the cortical sheet. Anatomical datasets were acquired using a T1-weighted MPRAGE sequence at an initial resolution of 0.9×0.9×0.9mm. After correcting the high-resolution T1 anatomical datasets for low-spatial-

frequency intensity variations and down-sampling to 1×1×1×mm, we used SPM5 (http://www.fil.ion.ucl.ac.uk/spm/) to align and average several complete 3D volumes to improve the signal-to-noise ratio. Initial segmentation of the white and gray matter was performed using the Freesurfer 4 '*autorecon*' script (http://surfer.nmr.mgh.harvard.edu/) and the results were then passed to the Stanford 'VISTA' toolbox (http://white.stanford.edu/software/) application '*mrGray*' where a human expert corrected small errors in the topology of the white matter to finalize both gray and white matter classifications. The resulting gray and white matter volumes were used to generate cortical surface meshes for data visualization (Teo, Sapiro et al. 1997).

Functional data preprocessing—T2* data were post-processed to remove intra- and inter-run motion artifacts using the rigid body alignment routine '*spm_coreg*' from SPM5. Reconstructed, motion-corrected time series were imported into the Stanford VISTA package and aligned to the high-resolution anatomy by registering the 'inplane' anatomy scans with the high-resolution anatomy and applying the resulting affine transform to the motion-corrected functional datasets. Automated alignment estimates were checked visually by human experts. BOLD signal changes were computed as percentage variations around the mean. Functional data were convolved spatially with a 2×2×2mm (FWHM) Gaussian filter and underwent a second-order polynomial detrending prior to the computation of the GLM.

Stimulus presentation—All visual stimuli were presented on a flat-panel LCD screen (LTV32W1, Westinghouse Electric Corp., Cranberry, Penn.) contained within an electromagnetically-shielded box and viewed at the rear of the scanner bore via a mirror mounted on the headcoil. The gamma lookup tables and spectra for each color channel were calibrated using a photoradiometer (USB2000, OceanOptics, FL) in order to ensure output linearity (Brainard 1989). Stimuli were generated using an in-house stimulus display package (PowerDiva) running on a G4 Mac Powerbook (Apple, Cupertino). The Powerdiva package was originally designed for quantitative measurements of EEG response functions and provides millisecond-resolution control over stimulus timing.

The LCD screen subtended a visual angle of seven degrees of visual angle horizontally. In most experiments, subjects performed a free-running, rapid letter discrimination task in the central half degree of the visual field, responding via a magnet-safe button box connected to a fiber-optic response pad (FORP FIU-005, Current Designs, PA) which converted button presses to signals on the Powerbook USB port. The letter discrimination task was based on one used by Schira *et al* (Schira, Fahle et al. 2004) in an fMRI study of contour processing. Sequences of randomly-rotated letters were presented in the order **F**,(**L** or **T**),**F**. The subject's task was to indicate as soon as possible whether the central portion of the sequence contained a '**T**' or not. The timing of the attentional control task was independent of the onsets and offsets of the stimulus gratings. Performance on the letter discrimination task was monitored by the display program and the rate of letter presentation was adjusted continuously to maintain a discrimination accuracy of 75% for all subjects. Typical letter presentation times were around 300ms. To control for the effect of spatial attention location, three subjects also participated in experiments where the annulus+mask NBR stimuli were identical to those described below but the free-running letter discrimination task was presented to the left and right of fixation within the annular surround. In this configuration, letters were presented in pairs and scaled to maintain the same discrimination accuracy measured for foveal presentations. Otherwise the task was identical.

Stimulus configuration—Initially, we measured the contrast dependency of the NBR using stimuli that contained only achromatic luminance contrast. The central 'inducer' region measured 1.5 degrees in diameter and was either set to zero contrast (uniform field of 35cd/m^2) or contained a 1cpd contrast-reversing sine-wave grating with a Michelson

contrast of 90% and a temporal frequency of 4Hz. The surround region contained a contrast-reversing sine-wave grating similar to that used in the central region except that its spatial phase was inverted and its Michelson contrast was set to one of four different levels: 0% (uniform mean field), 5%, 20% or 45%. To eliminate border contrast effects and top-down influences due to segmentation state, a 0.25 degrees annulus between the central inducer and the surrounding probe region was always set to a uniform mean gray (Figure 2a). The lowest non-zero probe contrast of 5% was above perceptual detection threshold when presented in isolation.

In a second set of experiments examining the chromatic tuning of the NBR, we used an identical spatial stimulus configuration and event-related paradigm for the central mask region but altered its chromaticity. Specifically, we ran two stimulus conditions in addition to a blank where the central contrast was defined by excursions along the (L+M+S) and (L −M)-cone directions in MacLeod-Boynton space (MacLeod and Boynton 1979) at RMS cone contrasts of 45% and 6% respectively. The first of these conditions was similar to the zero-surround-contrast condition in our first dataset. The second condition drove the central region with a grating that was highly-salient but nominally isoluminant. No peripheral grating was present in these experiments. Cone isolating stimuli were computed using a ‘silent substitution’ technique (Estevez and Spekreijse 1982) based on the measured spectra of the display device and published measurements of the human cone photoreceptor absorption spectra in the central retina (Stockman, MacLeod et al. 1993).

Experimental design—Stimuli were presented in a jittered event-related paradigm (Burock, Buckner et al. 1998) with a two second stimulus duration, a nine second mean inter-stimulus interval (ISI) with a random jitter drawn from a uniform distribution spanning +/− six seconds. Each fMRI run lasted 368 seconds including a six-second scanner ‘warm-up’ period during which no stimulus was present and an additional six-second lead period to avoid measuring the attentional correlates of the initial stimulus onset transients. Eight different stimulus conditions were presented within this period representing all the combinations of the four probe contrasts (0%, 5%, 20%, and 45% contrast), and the two central inducer contrasts (0%, and 90% contrast). Each condition appeared four times per run and each subject completed a minimum of seven runs.

Localizer stimuli—Prior to running the event-related experiments, we performed a series of block-design experiments using high-contrast stimuli with a spatial structure identical to those in the event-related paradigm in order to identify the borders of the foveal and parafoveal regions. The regions of interest defined by these experiments (defined as regions that were significantly active at $p<0.0001$ in a correlation analysis (Bandettini, Jesmanowicz et al. 1993)) were automatically eroded by one voxel in order to avoid locations close to the borders where induced contrast effects may have been present (Cornelissen, Wade et al. 2006). In addition, on a third occasion, we ran standard retinotopic mapping experiments in order to identify the boundaries of early visual areas (Sereno, Dale et al. 1995; DeYoe, Carman et al. 1996). These localizer experiments were conducted at least one week before the event-related measurements. The data shown here are all from area V1 averaged across hemispheres in each subject.

Analysis methods—Event-related analyses, including application of general linear models and hypothesis tests to generate contrast maps, were performed as described by Frackowiak *et al* (Frackowiak, Friston et al. 2003) and Dale and Buckner (Dale and Buckner 1997). These analysis routines are part of the VISTA package and provide essentially identical results to the equivalent routines in SPM5 (Sayres and Grill-Spector 2006). Predictor time series estimates were generated by applying a canonical SPM5 ‘difference of gammas’ hemodynamic response function to the stimulus onset times. No other regressors

(for example, estimates of motion-induced noise) were incorporated in the analysis. In this study, we estimate the BOLD response amplitudes as being proportional to the fitted GLM beta values. Other measures of BOLD amplitude (for example, mean peak height at some lag after stimulus onset) were found to yield similar but slightly less robust estimates of BOLD response. Curve fitting and statistical analysis of the population response amplitudes were performed in Matlab (Mathworks, Natick, MA) using the statistical analysis toolbox and optimization toolboxes. We used a version of the Matlab '*fminsearch*' unconstrained multidimensional minimization algorithm to find solutions to our parameter fits that were optimal in a weighted least-squares sense. Because this algorithm can find minima that are locally- but not globally-optimal, we repeated each search at least 100 times with different start values in order to find a stable solution.

Psychophysical methods

Subjects—Five subjects (three males) with ages between 30 and 38 (mean 35) participated in our psychophysical experiments. All subjects had normal or corrected-to-normal acuity, normal color vision and were experienced psychophysical observers. Three of the subjects were naïve to the purpose of the experiment. Subjects were screened and consented in accordance with human subject protocols at both the University of California, San Francisco (UCSF), and the Smith-Kettlewell Eye Research Institute (SKERI). Three of the psychophysical subjects were also subjects in the fMRI experiments.

Stimulus presentation—Stimuli were presented on a Sony Multiscan 200 CRT monitor (mean luminance 34cd/msq, 100Hz refresh rate, 1024×768). Subjects viewed the stimuli binocularly at a distance of 70cm in a darkened room and responded to the two-alternative forced-choice psychophysical tests by pressing one of two keys on the stimulus computer keyboard. The screen was calibrated and linearized with the same photoradiometer used in the fMRI experiments (USB2000, OceanOptics, FL).

Stimulus configuration—The stimulus parameters were matched as closely as possible with those used in the fMRI experiments and in particular the spatial configurations of the stimuli in the two experiments were identical: a central disk surrounded by an annulus with a mean-luminance gap between them. Subjects were instructed to perform two-temporal-interval, two alternative forced-choice contrast modulation detection decisions in all experiments. In half of the experiments, the judgments were made on the contrast of the central disk. In the other half of the experiments, judgments were made on the contrast of the annulus. In both conditions, a staircase routine (Watson and Pelli 1983) was used to determine the 78% contrast modulation detection threshold in the target location. By varying the pedestal contrast of both regions from session to session, we were able to collect threshold-versus-contrast (TVC) curves for each subject. In total, we collected four such TVC curve for each subject corresponding to each of the two target locations presented with, and without the other half of the stimulus (disk alone, disk + high-contrast annulus, annulus alone, annulus + high-contrast disk). Contrast detection thresholds can be related to neural responses by assuming that the responses they generate correspond to signal changes equal to either a constant, or Poisson neural noise level (Foley 1994; Boynton, Demb et al. 1999; Itti, Koch et al. 2000; Dayan and Abbott 2001). We were therefore able to compute the effects of central and parafoveal maskers on the neural activity underlying the contrast discrimination judgments.

Results

fMRI

Long-range neural suppression in the visual system is a well-studied phenomenon and there are several candidate models of this process that have plausible physiological explanations. On first inspection, the NBR would appear to be related to a phenomenon known as 'surround suppression'. Surround suppression refers to a cascade of normalization processes in the early visual system that cause neuronal firing rates and psychophysical detection and appearance measurements to be modulated by contrast presented outside the classical receptive field (Blakemore and Tobin 1972; Allman, Miezin et al. 1985; Cavanaugh, Bair et al. 2002). The link between psychophysical surround suppression and electrophysiological measurements of extraclassical receptive field modulation is still a subject of investigation. However, there is convergent evidence from several studies indicating that surround suppression consists of at least two components: an early, broadly-tuned suppressive mechanism acting at or before the input layer of V1, and a later, more tightly-tuned cortical mechanism that may involve feedback from extrastriate visual areas (Webb, Dhruv et al. 2005; Angelucci and Bressloff 2006; Petrov and McKee 2009).

Recent multimodal experiments in primary somatosensory cortex, have made the link between neural suppression and the NBR more concrete. In particular, in an elegant series of studies, Devor *et al* (Devor, Tian et al. 2007) showed that the NBR around a stimulated location is associated with arteriovascular constriction and a decrease in membrane potential (a hyperpolarization) in the surround (see also (Derdikman, Hildesheim et al. 2003; Devor, Ulbert et al. 2005)). Interestingly, this hyperpolarization did not appear to be associated with a significant reduction in multiunit spike activity in the same location, nor was it associated with a change in local glucose uptake, which reflects the local metabolic rate (Devor, Hillman et al. 2008).

The mean membrane hyperpolarization measured by Devor et al using voltage sensitive dye (VSD) is relatively small (around 0.1% of the mean) but modulations of this magnitude have been reported in correlated cell populations where the individual units demonstrate hyperpolarization effects of 10% or more (Grinvald, Shoham et al. 2001). The effects seen by Devor *et al* could therefore be comparable, at a single unit level, to other well-known suppressive mechanisms associated with membrane hyperpolarization — contrast adaptation being the most obvious example (Carandini and Ferster 1997).

How does the nature of the suppression induced by the high-contrast center vary as a function of baseline activity? This question is the key to understanding the link between neural suppression, the NBR and perception. We examined this relationship by manipulating the ongoing activity in a probe region, and then modulating the BOLD response generated in that location by presenting a high-contrast central masker. The change in the parafoveal BOLD response reflects the amount of neural modulation generated by the masker at each contrast level C_s presented to the probe region. By comparing the 'response versus contrast' (RVC) functions in the suppressed and unsuppressed conditions we were able to determine how suppression depends upon ongoing activity at a population level. We tested three common models of neuronal gain control. Following convention, we term these '*subtractive*', '*contrast gain*' and '*response gain*' mechanisms (Figure 1).

In a subtractive or 'baseline shift' model (Figure 1a), the response of the suppressed region is changed by a constant amount. Subtractive mechanisms are a fundamental part of early visual system contrast processing (Movshon, Thompson et al. 1978; Palmer and Davis 1981; Ferster 1988) and this type of response modulation has also been shown to be a good

(Buracas and Boynton 2007) or partial (Li, Lu et al. 2008) fit for BOLD modulation due to spatial attention in primary visual cortex.

The response gain model (Figure 1b) predicts that suppression scales with ongoing probe activity — causing monotonically-increasing absolute levels of suppression with increasing C_s. Response gain models have been used to explain response changes measured in single units in response to contrast or size changes (Solomon, White et al. 2002), shifts in spatial attention (Williford and Maunsell 2006) or adaptation (Ling, Liu et al. 2008).

The third candidate model, the contrast gain model (Figure 1c), predicts that the inducer scales the effective input contrast in the probe region. In this case, we find a suppression function that can be non-monotonic and depends on the precise form of the underlying contrast response function. This type of gain control is ubiquitous in the visual system (Heeger 1992) and is frequently proposed as a candidate for long-range suppressive interactions (Cavanaugh, Bair et al. 2002; Cavanaugh, Bair et al. 2002) as well as other, higher-level effect such as attentional modulation (Treue and Martinez Trujillo 1999; Boynton 2009; Reynolds and Heeger 2009).

To study the computational nature of the NBR in primary visual cortex, we used fMRI to measure contrast vs response functions (CRFs) in an annulus surrounding the fovea. These CRFs were measured both with and without a central, circular, high-contrast ‘inducer’. The regions of interest (ROIs) used to extract signals from visual cortex were defined using independent localizer scans and restricted to retinotopically-defined striate cortex (see Methods).

Our event-related design measured the effect of the NBR at four different levels of contrast (C_s) in the annular probe region (0%, 5%, 20%, 45%) and two levels of foveal inducer contrast (0% and 90%). Therefore, we measured a total of eight conditions allowing us to fit CRFs in the probe region with and without the high-contrast suppressor. The spatial stimulus configuration used in all experiments was similar to that shown in Figure 2.

Figure 3 shows the mean BOLD response amplitudes in the inducer (3a,c) and probe regions (3b,d) computed from a general linear model fit of the fMRI timeseries data in each ROI at all combinations of inducer and probe contrast levels. Results from all subjects are shown in 3a and 3b, average results with cross-subject SEMs are shown in 3c,d. The patterns of individual results were similar in all subjects, as reflected by the SEM error bars for the group average BOLD amplitudes.

We defined the NBR to be the change in BOLD signal due to the presence of the high-contrast central region. This value was calculated as the difference of BOLD response amplitudes in the probe ROI between corresponding conditions with and without the inducer. The NBR associated with each background contrast is shown in Figure 3e.

The most striking aspect of the data shown in Figure 3 is that the amplitude of the NBR falls rapidly with increasing probe contrast and is maximal at 0% probe contrast (corresponding to a uniform mean field in the parafovea). Clearly, the NBR is not independent of the probe contrast level. This finding strongly rules against the subtractive response model because this predicts approximate independence between the NBR and C_s. Fitting a pure subtractive model yields an R^2 (percentage of variance explained, computed as 1-[var(*residuals*)/ var(*data*)]), of zero. The response gain model can be rejected even more conclusively since it predicts that the NBR should increase monotonically with probe contrast. Again, the best fit of this model has a zero R^2, meaning that it explains no significant amount of the variance. Intuitively, neither the subtractive model nor the response gain model can fit the data better than a flat line.

A contrast gain model, however, fits the data well. Specifically, we fit a hyperbolic ratio of the form

$$r=\frac{k(sc+c_0)^m}{\sigma^m+(sc+c_0)^m}+A \quad \text{Equation 1}$$

to the data (Albrecht and Hamilton 1982). This type of saturating non-linearity has often been used to fit both neural (Albrecht and Hamilton 1982; DeAngelis, Freeman et al. 1994; Cavanaugh, Bair et al. 2002; Durand, Freeman et al. 2007) and fMRI (Boynton, Demb et al. 1999; Wade and Wandell 2002) response data. We fit all eight data points simultaneously by minimizing a single function that computed the suppressed and unsuppressed responses at each contrast level. We fixed two parameters (the exponent *m* and a multiplicative contrast gain control scalar *s*, set to 1 for the unsuppressed condition and 0.62 in the suppressed condition, that alters the effective input contrast). We allowed four parameters to vary: k (response gain), σ (semi-saturation constant), *A* (an offset at zero contrast) and C_0 (an estimate of baseline neural input). The exponent 'm' was fixed at the value of 2 commonly used in the literature to model population responses (e.g. (Boynton, Demb et al. 1999; Chirimuuta and Tolhurst 2005)) and the multiplicative suppression factor *s* of 0.62 was based on population data from Cavanaugh *et al* (Cavanaugh, Bair et al. 2002) and equivalent to their mean measured suppression index $(R_{max}-R_{min})/R_{max}$ of 0.38. Our results do not depend critically upon these values. For example, changing the exponent to the value of 1.8 derived from experimental data by Boynton et al (Boynton, Demb et al. 1999) had little qualitative effect on our results. All eight data points contributed to the fit. For the additive and response-gain models, we did not have existing population estimates of neural suppression and so we allowed this value to vary as an additional parameter, adjusting our chi-squared estimates later to account for the additional degree of freedom.

The fitted parameters and the associated curve fits are shown in Figure 4. Although the fit slightly underestimates the NBR at low probe contrast and may overestimate it at high contrast, they explain a significant amount of the variance in our data (R^2=0.87) and the parameters are physiologically-plausible and lie well within their maximum and minimum bounds.

In order to compare the three models in a more quantitative manner, we computed F-statistics on the reduced chi-squared values for each fit type taking into account the number of degrees of freedom in each model. The contrast gain model provided the best fit of the three model types and was superior to the response gain model ($p>0.98$). The comparison between the contrast gain model and the subtractive (constant difference) model also achieved statistical significance ($p>0.95$) in this relatively rigorous test. The failure of the subtractive model to explain any fraction of the variance (R^2=0) leads us to reject it even more conclusively as a possible mechanism.

Although the suppressive response can, in principle, be due to a combination of several mechanisms (See (Li, Lu et al. 2008)) for a thorough treatment of this type of mixed model), the very low magnitude of the NBR at moderately-high C_s, and the lack of any NBR at near-saturating 45% contrast, argues strongly against either a subtractive or a response-gain component and we did not consider these potential mechanisms further.

In addition to making clear distinctions between the three potential suppressive mechanisms, these results also have two other important features.

Firstly, we discovered that the *negative* BOLD response may be as large in magnitude as a strongly elicited *positive* BOLD response. For example, the maximum NBR in the probe (Figure 3c, first data point) is comparable in absolute magnitude to the PBR in the same

location elicited by a near saturating 45% contrast grating (Figure 3d, C_s=45%). This suggests that the resting-state BOLD signal in the presence of a completely blank mean-gray screen in parafoveal V1, is at least half of the maximum possible response in that region. In other words, although it is normally considered to be a baseline signal, the BOLD level associated with blank screen of constant luminance is well above absolute zero in peripheral striate cortex.

Secondly, although a strong NBR is elicited by the foveal inducer in the surround (Figure 3d), there is no detectable NBR in the foveal region in response to a high contrast parafoveal stimulus. Figure 3c shows the response in the inducer region as a function of surround contrast. The bottom row of data points are measures of BOLD amplitude at 0% inducer contrast and the right-most point in this series indicates the BOLD amplitude in the presence of a high-contrast (45%) surround. The amplitude for this condition is not statistically different from zero, or from the amplitudes at other surround contrasts. In other words, the contrast gain control mechanism responsible for the parafoveal NBR appears to be much weaker in the fovea.

As noted above, the NBR appears to reflect the average degree of membrane hyperpolarization in the surround rather than the direct neural spike rate (Devor, Tian et al. 2007) or energy consumption (Devor, Hillman et al. 2008). Although neuronal spiking clearly depends on membrane potential in any particular neuron, the relationship may be obscured by threshold effects (Priebe, Mechler et al. 2004; Priebe and Ferster 2008) and the fact that only some of the neurons in the probe actually experience suppression (Solomon, White et al. 2002). Equation 1 may therefore predict qualitative changes in the membrane polarization and the spike rate of a small subpopulation of cortical neurons in the suppressed region.

Because all the experiments described above used an attentional control task presented in the fovea, we were concerned that the lack of NBR in the fovea might simply be due to a high baseline activation level in this location (Heinemann, Kleinschmidt et al. 2009). To control for this, we ran additional control experiments on a subset of our subjects. Firstly, we ran a version of the experiment that was identical to that described above except that the attentional control task was presented in the annular probe. The results of this experiment are shown in Figure 5. As before, we measured a strong NBR in the parafovea and no NBR in the fovea for any condition. As a second control, we ran a block-design version of the experiment with no attentional control at all. Results from this experiment likewise showed a parafoveal NBR but no foveal NBR (See Supplementary Figure S1). Based on the results from these attentional controls, we believe that the relative weakness of the foveal NBR is a fundamental property of the human visual system.

The weakness of the NBR in the fovea led us to hypothesize that it may be generated in only a subset of cortical or subcortical neurons – a subset that may be relatively sparse in the fovea. A natural candidate was the magnocellular pathway. Single unit studies have demonstrated that extraclassical, suppressive receptive fields are far stronger in the magnocellular pathway than in the parvocellular pathway (Barlow, Derrington et al. 1977; Solomon, Peirce et al. 2004; Solomon, Lee et al. 2006). While the fovea is dominated by parvocellular input, the ratio of parvo to magnocellular cells falls rapidly with increasing eccentricity (Connolly and Van Essen 1984; Azzopardi, Jones et al. 1999). We propose that it is this ratio (rather than the absolute number of foveal magnocellular neurons) that is critical to the amplitude of the NBR. Devor and colleagues model the NBR as the result of a linear combination of a positive response and a negative response. It is clear from many fMRI studies of chromatic responses in V1, including one shown later in this paper, that both the parvocellular and magnocellular pathways are capable of generating a positive

BOLD response but it is possible that the negative response, at least in this stimulus configuration, is generated only by the magnocellular cells.

If the NBR was predominantly associated with magnocellular neurons in the early visual pathways, we would expect to find little or no NBR generated by isoluminant stimuli since there is relatively little isoluminant input to the magnocellular pathway (Lee and Sun 2009). In order to test this hypothesis, we conducted a set of experiments where we compared the amount of NBR generated in the parafovea by a) achromatic luminance and b) isoluminant red-green gratings in the fovea. We analyzed these data using the same data-processing pipeline that we used for the event-related luminance-contrast datasets in Figure 3 and Figure 4. We then compared the levels of positive and negative BOLD signals in the foveal, stimulated regions and the parafoveal, unstimulated regions. The results are shown in Figure 6.

In all subjects, both the luminance-contrast and isoluminant stimuli generated strong, positive, central responses. The responses due to the achromatic (45%) and isoluminant (6%) gratings were approximately equal, meaning that the isoluminant cone stimuli were slightly less than eight times more effective per unit cone contrast at driving BOLD signals in V1 – a result that is consistent with many other fMRI studies of chromatic responsivity (Kleinschmidt, Lee et al. 1996; Engel, Zhang et al. 1997; Wandell, Poirson et al. 1999; Liu and Wandell 2005). The contrasts for the (L+M+S)-cone and (L−M)-cone stimuli were selected to equalize the resulting BOLD responses, but this compensation was not perfect and our foveal (L−M)-cone driven responses were, on average, slightly larger than the (L+M +S)-cone signals. Since the magnitude of the NBR is proportional to the contrast of the inducer (Shmuel, Augath et al. 2006), we might expect these isoluminant stimuli to generate an equally-robust NBR. Strikingly, however we found that while the foveal luminance stimuli generated a powerful NBR in the parafovea, the isoluminant (L−M)-cone stimuli generated a far-weaker suppressive effect. This statistically significant ($p<0.01$, one-sided t-test) reduction in the amplitude of the NBR for the parvocellular pathway was particularly striking when the NBR was expressed as a fraction of the positive response (PBR) elicited by these stimuli in the fovea. On average, the ratio of positive to negative responses for the luminance contrast stimuli was 0.61. For the isoluminant stimuli it was 0.37. We note that the contrast levels used for this stimulus were potentially high enough to cause saturation of both the luminance- and isoluminant contrast-driven responses that would, in turn, diminish the strength of the effect we measured. In addition, our chromatic stimuli were generated based solely on computed cone absorption values rather than individually-set isoluminant points and were presented on an eight-bit display device. Consequently, there may have been some luminance artifact in our nominally (L−M)-cone isolating gratings, although this artifact must have been relatively small given the low absolute cone contrasts in this condition. In the supplementary material (S2), we show additional data that we derived from a re-analysis of the Liu and Wandell dataset (Liu and Wandell 2005) which measured responses to attentionally-controlled chromatic stimuli very similar to our own where spatial dithering was used to improve the apparent color bit-depth. The analysis procedures were identical to those described above and the average contrast of the stimuli was approximately half that of those shown in Figure 6. The reduction in the relative amplitude of the isoluminant (L−M)-cone-driven NBR is even more prominent in these data.

Psychophysics

The fMRI results above indicate a clear pattern of BOLD signal suppression in the parafovea due to a central, high-contrast target while high-contrast parafoveal targets do not appear to generate significant suppression in the fovea. If these suppressive effects have a neural origin, they might have perceptual correlates that could be detected using behavioral psychophysics.

To examine this, we ran a series of psychophysical experiments to measure the neural response functions underlying contrast detection and discrimination in the fovea and parafovea with and without high-contrast, spatially-remote mask regions. The stimuli were chosen to match those used in the fMRI experiments. We used a two-interval, two-alternative forced-choice paradigm (2AFC) to measure contrast discrimination threshold-vs-pedestal contrast (TVC) functions in both foveal and parafoveal locations. We then computed response vs contrast (RVC) functions by assuming that discrimination thresholds corresponded to neural response differences that were larger than some criterion noise level (Foley 1994; Dayan and Abbott 2001). The data in Figure 7 were computed by assuming a Poisson-distributed noise model (Itti, Koch et al. 2000; Dayan and Abbott 2001) plus a small baseline component at zero contrast. In a separate analysis, we also computed RVC curves using an alternative detection algorithm with a constant noise level, corresponding to a limit at some more central decision stage (Shadlen, Britten et al. 1996) and the results were qualitatively similar. Figure 7 shows the raw TVC curves obtained in the fovea (a) and parafovea (b). Data points measured using isolated, unmasked probes are shown in black, data points measured in the presence of a high-contrast, spatially-remote suppressive field are shown in gray. Three aspects of the data are worth noting. Firstly, there is little or no effect on foveal contrast discrimination thresholds of adding a high-contrast annular surround. This result extends a finding by Petrov *et al* (Petrov, Carandini et al. 2005) which found no evidence for surround suppression in a foveal target using a contrast detection paradigm. In their paper, Petrov *et al* measured suppression using contrast detection thresholds at zero pedestal contrast. We confirm this original result using very similar stimuli and show that it extends across a wide range of pedestal contrasts. Similar, though less pronounced peripheral bias effects have also been noted in contrast appearance measurements (Xing and Heeger 2000; Xing and Heeger 2001).

Secondly, we do find evidence of threshold changes in the parafoveal annulus in response to the presence of high-contrast foveal mask. Since this configuration essentially replicates the conditions used in our fMRI experiment, the psychophysical data parallel the fovea/parafovea bias that we observe in the NBR.

Finally, the computational nature of the suppression that gives rise to the increase in psychophysical detection thresholds is different to that seen in the NBR data. Specifically, the increase in contrast discrimination thresholds at high pedestal levels indicates the presence of a response- rather than a contrast-gain control mechanism. This is illustrated in Figure 7c where the underlying neural contrast response functions for the suppressed and unsuppressed parafoveal probes are computed. The fitted curves are hyperbolic ratio functions with two free parameters: k and sigma. The same parameters were used to generate the fits in Figure 7b.

How can the response gain that we observe psychophysically be reconciled with the contrast gain control that we observe in the fMRI BOLD signal?

We believe that there are at least three possible explanations.

1: This may be an early effect limited to a relatively small population of magnocellular neurons that saturate at low contrast. At higher contrasts, response gain may occur in a different set of neurons, possibly a parvocellular-dominated population.

2: Tuned versus untuned suppression. It is becoming clear that that psychophysical surround suppression is an umbrella term describing the cumulative result of at least two physiological processes. Long-range suppressive effects are found in the lateral geniculate nucleus (Bonin, Mante et al. 2005) and even in the retina (Solomon, Lee et al. 2006) but these mechanisms are relatively untuned for spatial features such as frequency and

orientation. Additional suppressive, and occasional facilitatory interactions are found in cortex and most likely result from a combination of untuned suppression at the input layers and rapid, highly-tuned feedback interactions from extrastriate cortex (Webb, Dhruv et al. 2005; Smith, Bair et al. 2006; Ichida, Schwabe et al. 2007). Surround suppression as it is usually measured psychophysically has a significant tuned component indicating a strong contribution from cortical neurons (Petrov, Carandini et al. 2005) although the early and late mechanisms can be dissociated to some degree by manipulating stimulus timing (Petrov and McKee 2009).

Electrophysiological studies of surround suppression indicate that it is implemented as a multiplicative contrast gain control change at the level of individual neurons (Webb, Dhruv et al. 2005). However its ultimate effect on perception depends on the way in which signals in individual neurons are combined and normalized prior to the decision stage. Visual signals are subject to a cascade of contrast normalization processes which act to adapt neuronal responses to the mean local contrast level (Heeger 1992; Carandini, Demb et al. 2005; Petrov, Carandini et al. 2005). These normalization stages are often described by a divisive computation similar to that shown in Equation 1 in which the output from each neuron is divided by the pooled response from its neighbors (Heeger 1992; Carandini, Heeger et al. 1997). When suppression is spatially untuned, the contrast in both the numerator and the divisor are reduced and the overall result can be described by a change in the semisaturation constant or, equivalently, a multiplicative change in input contrast. By comparison, if the suppression is highly-tuned so that it affects only the numerator, the result can be modeled as a multiplicative change in output, or a ‘response-type’ gain change. This observation has been proposed recently to explain the wide variation in gain mechanisms observed in experiments studying attentional modulation (Reynolds and Heeger 2009). However, its general logic applies to any modulatory neural mechanism: suppression that is highly tuned, either for features or spatial location, will manifest as response gain after a divisive normalization stage, while broadly-tuned suppression resembles a contrast gain mechanisms. The response-type gain in our behavioral measurements may reflect the presence of a highly-tuned cortical feedback mechanism operating after the neural generator of the NBR. Consistent with this hypothesis, we found that psychophysical suppression of a high-contrast parfoveal probe due to a foveal mask was abolished if the orientation of the gratings in the mask and the probe were orthogonal. It is also worth noting that similar experiments using slightly different stimulus configurations report a suppressive modulation more consistent with a contrast gain control mechanism (Xing and Heeger). It is possible that these differences reflect subtle differences in spatial features, such as size and frequency, of individual stimulus components as well as the psychophysical task.

3: It may be that the NBR simply does not have a straightforward relationship to perception. Spikes are the only way to propagate information about the magnitude of visual attributes. A phenomenon that does not have a direct effect on spiking rate (Devor, Tian et al. 2007) may, therefore, perform some role that is not easily-detected in our psychophysical measures of contrast vs neural response. One candidate may be a relatively automatic de-allocation of hemodynamic resources in the parafovea in anticipation of a long-term reduction in activity there (Sirotin and Das 2009).

Discussion

We have shown that the NBR in a region of primary visual cortex representing the parafovea (1.5° – 3°) can be modeled as a multiplicative gain control mechanism with a large zero-contrast response offset. The NBR in the parafoveal region is greatest at zero probe contrast (where the modeled contrast response function is steep) and reduced at higher probe contrast due to a combination of response saturation and, possibly, the increased contribution of a

population of neurons that have more linear response functions and which do not undergo long-range suppression to the same degree. Intriguingly, we found little evidence of a similar type of NBR in the fovea and we also found that isoluminant chromatic contrast generates relatively little NBR.

We found that the NBR is induced at parafoveal cortical locations during foveal stimulation but that at the resolution of our measurement and under conditions of zero foveal contrast, more peripheral stimulation generates little or no NBR in the foveal representation of V1. In other words, the neural suppression has a well-defined spatial direction on cortex. This asymmetry is evident in our own raw amplitude response maps of primary visual cortex and in other published studies. A striking example can be seen in Figure 2 of a paper by Duncan and Boynton (Duncan and Boynton 2003) (See also Supplementary material Figure S3) where the negative BOLD response to various high-contrast ring stimuli is always on the side furthest from the fovea.

Why do we not measure an NBR in the fovea similar to the one found in the parafovea? One reason might be the differential sensitivity of parvo- and magno-cellular cells to suppression from outside their classical receptive fields. It has been shown that parvocellular cells (which dominate the fovea (Azzopardi, Jones et al. 1999) exhibit far less extraclassical inhibition than magnocellular cells (Kruger 1977; Solomon, White et al. 2002). The amplitude of the NBR in any location must depend upon the ratio of suppressed to unsuppressed neurons and this, coupled with the steeply-varying ratio of parvo- to magnocellular cells across the visual field would predict its relative reduction in the fovea. Intriguingly, human behavioral studies (including our own) have shown that surround suppression is either reduced (Xing and Heeger 2000) or absent (Petrov, Carandini et al. 2005) when the probe region is presented in the fovea.

Recent work suggests that at least two mechanisms are involved in this surround suppression: an ‘early’ mechanism that is relatively untuned for spatial frequency and which may act at the first synapse of V1 and a later mechanism which has sharper spatial frequency tuning and which may involve an extrastriate feedback loop (Angelucci, Levitt et al. 2002; Bair, Cavanaugh et al. 2003; Webb, Dhruv et al. 2005). We believe that the NBR is most likely to reflect the action of the ‘early’ suppressive mechanism which may also drive the type of long-range, perceptual suppression measured using short-duration, low-contrast probes in the periphery (Petrov, Carandini et al. 2005).

The spatial bias is also intriguing for another reason. One high-level manifestation of long-range spatial interactions is the phenomenon of ‘crowding’: a decrement in letter or orientation discrimination in the presence of adjacent contrast that may be related to surround suppression although perhaps not identical to it (Petrov, Popple et al. 2007). Crowding, like the NBR and surround suppression, is present in the periphery but not the fovea of normal observers. When measured in the periphery, it has an inward bias (Petrov, Popple et al. 2007) meaning suppression from more eccentric masks tend to be more effective. The direction of this local bias appears to be the opposite of that seen in the NBR but the situation may be complicated by computational considerations relating to the effect of contrast gain control on different tasks.

The BOLD contrast response function in the parafovea has a large offset at zero contrast. The magnitude of the NBR measured to date in other studies confirms this high ‘resting-state’ BOLD level since all these studies measure a robust NBR on a blank mean-field (Shmuel, Yacoub et al. 2002; Smith, Williams et al. 2004; Shmuel, Augath et al. 2006). In our experiments, it is especially striking that when an NBR is induced in a zero-contrast parafoveal location, the magnitude of the BOLD response decrease is comparable to that of

the positive response elicited by a near-saturating 45% contrast grating. It is important to note that this high baseline BOLD offset is not an artifact of any of our models or fitting procedures. It is required by the observation that the magnitude of the NBR on a blank background is relatively large. This large underlying baseline signal cannot be explained by a linear relationship with neural spiking activity since spontaneous spike rates in V1 neurons are typically no more than 10% of the maximum (Albrecht and Hamilton 1982).

If, as has been suggested, the BOLD activity reflected pre-synaptic mechanisms such as DC offsets in membrane potential (Logothetis and Wandell 2004; Devor, Tian et al. 2007), the range of variation could be much greater. Moreover, the large NBR that is measured at zero-contrast does not imply an equally large change in local energy consumption. Devor and colleagues have shown that in rat somatosensory cortex, arteriovascular constriction associated with decreases in membrane potential are not associated with a reduction in glucose uptake (Devor, Hillman et al. 2008). While the relationship between energy use and membrane potential may be stronger in regions with higher baseline firing rates (for example, primate V1), this result suggests that changes in the local, mean membrane potential may alter blood flow and oxygenation without significantly affecting population firing rates. This observation in itself hints that the NBR may not be directly related to perception and similar effects may underlie recent reports of hemodynamic changes in the absence of a visual stimulus (Sirotin and Das 2009).

One alternative hypothesis is that the baseline BOLD response in the parafovea may be driven by the constant mean-gray background. It is possible, for example, that responses are driven by the ‘luxotonic’ class of cells reported by Kayama and colleagues (Kayama, Riso et al. 1979) although these cells appear to be relatively rare and there is no evidence that they are restricted to a particular eccentricity. Another explanation is that the parafovea may be more sensitive to the rapid flicker of our fluorescent monitor backlight. While some cells in macaque visual cortex can follow flicker up to a frequency of 100Hz (Williams, Mechler et al. 2004; Logothetis, Murayama et al. 2009) and the periphery is certainly more sensitive to high frequency flicker than the fovea (McKee and Taylor 1984; Tyler and Hamer 1990; Tyler and Hamer 1993; Horiguchi, Nakadomari et al. 2009), the degree of entrainment is far higher when spatial contrast is present. Using a photocell and oscilloscope, we measured almost zero flicker in our LCD display below 100Hz during a mean field and we believe that it is unlikely that the small neural population that may be entrained (although not necessarily driven to spike more) above this frequency could drive the large offsets in BOLD signal that we observe.

The effect we measure is not due to an attentional mechanism. It is known that attention can modulate the BOLD signal in visual cortex by a significant amount (Tootell, Hadjikhani et al. 1998; Kastner, Pinsk et al. 1999; Ress, Backus et al. 2000; Buracas and Boynton 2007; Sirotin and Das 2009) and it is conceivable that the NBR also reflects allocation of attentional resources (Heinemann, Kleinschmidt et al. 2009). However, we controlled for the effect of attention in these experiments by forcing the subjects to perform a demanding letter discrimination task that was adjusted throughout the experimental session to maintain a 75% detection rate. Our result did not depend on the location of the attentional task. When we compared the effect of using foveal versus parafoveal attentional controls, we found no difference between the two conditions. Finally, our data are qualitatively similar to those obtained by other researchers (Shmuel, Yacoub et al. 2002; Shmuel, Augath et al. 2006; Devor, Tian et al. 2007) in anaesthetized animals where the effects of attention are absent.

These previously-unreported features of the NBR may have important consequences for the way we interpret fMRI data in early visual cortex. For example the spatial asymmetry in the NBR may have important consequences for experiments that aim to relate the positions of

stimuli presented in visual space to the locations of the corresponding BOLD responses in cortex. Such measurements often attempt to fit a symmetric Gaussian function to the instantaneous BOLD response, or fit a cosine function to the BOLD response timecourse generated by a 'traveling wave' of activity passing across cortex (Sereno, Dale et al. 1995; Engel, Glover et al. 1997). Because the signals near the fovea are combinations of spatially-*symmetric* positive activations and spatially-*asymmetric* negative responses, these fitting procedures will slightly, but systematically under-estimate the eccentricity of peripheral stimuli in cortical space. These effects will be particularly important when generating and comparing models of cortical magnification functions derived from fMRI (Baseler, Brewer et al. 2002; Duncan and Boynton 2003; Schira, Wade et al. 2007).

Supplementary Material

Refer to Web version on PubMed Central for supplementary material.

Acknowledgments

Funded by RO1EY013157, RO1 EY017071 and BCS0719973. We thank Matteo Carandini, Suzanne McKee, Anthony Norcia, Yury Petrov and Justin Ales for helpful discussions in the writing of this paper. Junjie Liu and Brian Wandell contributed the datasets for Figure S2. The figure in S3 was reproduced with permission from the authors.

References

Albrecht DG, Hamilton DB. Striate cortex of monkey and cat: contrast response function. J Neurophysiol. 1982; 48:217–237. [PubMed: 7119846]

Allman J, Miezin F, McGuinness E. Stimulus specific responses from beyond the classical receptive field: neurophysiological mechanisms for local-global comparisons in visual neurons. Annu Rev Neurosci. 1985; 8:407–430. [PubMed: 3885829]

Angelucci A, Bressloff PC. Contribution of feedforward, lateral and feedback connections to the classical receptive field center and extra-classical receptive field surround of primate V1 neurons. Prog Brain Res. 2006; 154:93–120. [PubMed: 17010705]

Angelucci A, Levitt JB, Lund JS. Anatomical origins of the classical receptive field and modulatory surround field of single neurons in macaque visual cortical area V1. Prog Brain Res. 2002; 136:373–388. [PubMed: 12143395]

Azzopardi P, Jones KE, Cowey A. Uneven mapping of magnocellular and parvocellular projections from the lateral geniculate nucleus to the striate cortex in the macaque monkey. Vision Res. 1999; 39:2179–2189. [PubMed: 10343800]

Bair W, Cavanaugh JR, Movshon JA. Time course and time-distance relationships for surround suppression in macaque V1 neurons. J Neurosci. 2003; 23:7690–7701. [PubMed: 12930809]

Bandettini PA, Jesmanowicz A, Wong EC, Hyde JS. Processing strategies for time-course data sets in functional MRI of the human brain. Magn Reson Med. 1993; 30:161–173. [PubMed: 8366797]

Barlow HB, Derrington AM, Harris LR, Lennie P. The effects of remote retinal stimulation on the responses of cat retinal ganglion cells. J Physiol (Lond). 1977; 269:177–194. [PubMed: 894539]

Baseler HA, Brewer AA, Sharpe LT, Morland AB, Jagle H, Wandell BA. Reorganization of human cortical maps caused by inherited photoreceptor abnormalities. Nat Neurosci. 2002; 5:364–370. [PubMed: 11914722]

Blakemore C, Tobin EA. Lateral inhibition between orientation detectors in the cat's visual cortex. Exp Brain Res. 1972; 15:439–440. [PubMed: 5079475]

Boas DA, Jones SR, Devor A, Huppert TJ, Dale AM. A vascular anatomical network model of the spatio-temporal response to brain activation. Neuroimage. 2008; 40:1116–1129. [PubMed: 18289880]

Bonin V, Mante V, Carandini M. The suppressive field of neurons in lateral geniculate nucleus. J Neurosci. 2005; 25:10844–10856. [PubMed: 16306397]

Boynton GM. A framework for describing the effects of attention on visual responses. Vision Res. 2009; 49:1129–1143. [PubMed: 19038281]

Boynton GM, Demb JB, Glover GH, Heeger DJ. Neuronal basis of contrast discrimination. Vision Res. 1999; 39:257–269. [PubMed: 10326134]

Brainard DH. Calibration of a computer controlled color monitor. Col Res Appl. 1989; 14:23–34.

Buracas GT, Boynton GM. The effect of spatial attention on contrast response functions in human visual cortex. J Neurosci. 2007; 27:93–97. [PubMed: 17202476]

Burock MA, Buckner RL, Woldorff MG, Rosen BR, Dale AM. Randomized event-related experimental designs allow for extremely rapid presentation rates using functional MRI. Neuroreport. 1998; 9:3735–3739. [PubMed: 9858388]

Carandini M, Ferster D. A tonic hyperpolarization underlying contrast adaptation in cat visual cortex. Science. 1997; 276:949–952. [PubMed: 9139658]

Carandini M, Heeger DJ, Movshon JA. Linearity and normalization in simple cells of the macaque primary visual cortex. J Neurosci. 1997; 17:8621–8644. [PubMed: 9334433]

Carandini M, Demb JB, Mante V, Tolhurst DJ, Dan Y, Olshausen BA, Gallant JL, Rust NC. Do we know what the early visual system does? J Neurosci. 2005; 25:10577–10597. [PubMed: 16291931]

Cavanaugh JR, Bair W, Movshon JA. Nature and interaction of signals from the receptive field center and surround in macaque V1 neurons. J Neurophysiol. 2002a; 88:2530–2546. [PubMed: 12424292]

Cavanaugh JR, Bair W, Movshon JA. Selectivity and spatial distribution of signals from the receptive field surround in macaque V1 neurons. J Neurophysiol. 2002b; 88:2547–2556. [PubMed: 12424293]

Chirimuuta M, Tolhurst DJ. Does a Bayesian model of V1 contrast coding offer a neurophysiological account of human contrast discrimination? Vision Res. 2005; 45:2943–2959. [PubMed: 16081128]

Connolly M, Van Essen D. The representation of the visual field in parvicellular and magnocellular layers of the lateral geniculate nucleus in the macaque monkey. J Comp Neurol. 1984; 226:544–564. [PubMed: 6747034]

Cornelissen FW, Wade AR, Vladusich T, Dougherty RF, Wandell BA. No functional magnetic resonance imaging evidence for brightness and color filling-in in early human visual cortex. J Neurosci. 2006; 26:3634–3641. [PubMed: 16597716]

Dale AM, Buckner RL. Selective Averaging of Rapidly Presented Individual Trials Using fMRI. Human Brain Mapping. 1997; 5:329–340. [PubMed: 20408237]

Dayan, P.; Abbott, LF. Theoretical neuroscience : computational and mathematical modeling of neural systems. Cambridge, Mass: Massachusetts Institute of Technology Press; 2001.

DeAngelis GC, Freeman RD, Ohzawa I. Length and width tuning of neurons in the cat's primary visual cortex. J Neurophysiol. 1994; 71:347–374. [PubMed: 8158236]

Derdikman D, Hildesheim R, Ahissar E, Arieli A, Grinvald A. Imaging spatiotemporal dynamics of surround inhibition in the barrels somatosensory cortex. J Neurosci. 2003; 23:3100–3105. [PubMed: 12716915]

Devor A, Ulbert I, Dunn AK, Narayanan SN, Jones SR, Andermann ML, Boas DA, Dale AM. Coupling of the cortical hemodynamic response to cortical and thalamic neuronal activity. Proc Natl Acad Sci U S A. 2005; 102:3822–3827. [PubMed: 15734797]

Devor A, Tian P, Nishimura N, Teng IC, Hillman EM, Narayanan SN, Ulbert I, Boas DA, Kleinfeld D, Dale AM. Suppressed neuronal activity and concurrent arteriolar vasoconstriction may explain negative blood oxygenation level-dependent signal. J Neurosci. 2007; 27:4452–4459. [PubMed: 17442830]

Devor A, Hillman EM, Tian P, Waeber C, Teng IC, Ruvinskaya L, Shalinsky MH, Zhu H, Haslinger RH, Narayanan SN, Ulbert I, Dunn AK, Lo EH, Rosen BR, Dale AM, Kleinfeld D, Boas DA. Stimulus-induced changes in blood flow and 2-deoxyglucose uptake dissociate in ipsilateral somatosensory cortex. J Neurosci. 2008; 28:14347–14357. [PubMed: 19118167]

DeYoe EA, Carman GJ, Bandettini P, Glickman S, Wieser J, Cox R, Miller D, Neitz J. Mapping striate and extrastriate visual areas in human cerebral cortex. Proc Natl Acad Sci U S A. 1996; 93:2382–2386. [PubMed: 8637882]

Duncan RO, Boynton GM. Cortical magnification within human primary visual cortex correlates with acuity thresholds. Neuron. 2003; 38:659–671. [PubMed: 12765616]

Durand S, Freeman TC, Carandini M. Temporal properties of surround suppression in cat primary visual cortex. Vis Neurosci. 2007; 24:679–690. [PubMed: 17686200]

Engel SA, Zhang X, Wandell B. Colour tuning in human visual cortex measured with functional magnetic resonance imaging. Nature. 1997a; 388:68–71. [PubMed: 9214503]

Engel SA, Glover GH, Wandell BA. Retinotopic organization in human visual cortex and the spatial precision of functional MRI. Cereb Cortex. 1997b; 7:181–192. [PubMed: 9087826]

Estevez O, Spekreijse H. The "silent substitution" method in visual research. Vision Res. 1982; 22:681–691. [PubMed: 7112962]

Ferster D. Spatially opponent excitation and inhibition in simple cells of the cat visual cortex. J Neurosci. 1988; 8:1172–1180. [PubMed: 3357015]

Foley JM. Human luminance pattern-vision mechanisms: masking experiments require a new model. J Opt Soc Am A Opt Image Sci Vis. 1994; 11:1710–1719. [PubMed: 8046537]

Frackowiak, RSJ.; Friston, KJ.; Frith, CD.; Dolan, M.; Price, C.; Zeki, K.; Ashburner, J.; Penny, WD. Human Brain Function. 2 Edition. Academic Press; 2003.

Grinvald, A.; Shoham, D.; Shmuel, A.; Glaser, D.; Vanzetta, I.; Shtoyerman, H.; Slovin, A.; Skerkin, C.; Hildesheim, R.; Arieli, A. Grodetsky Center for Research of Higher Brain Functions - Technical Report. Weizmann Institute; 2001. In-vivo Optical imaging of cortical architecture and dynamics.

Harel N, Lee SP, Nagaoka T, Kim DS, Kim SG. Origin of negative blood oxygenation level-dependent fMRI signals. J Cereb Blood Flow Metab. 2002; 22:908–917. [PubMed: 12172376]

Heeger DJ. Normalization of cell responses in cat striate cortex. Vis Neurosci. 1992; 9:181–197. [PubMed: 1504027]

Heinemann L, Kleinschmidt A, M√°ller NG. Exploring BOLD Changes during Spatial Attention in Non-Stimulated Visual Cortex. PLoS One. 2009; 4:e5560. [PubMed: 19440362]

Horiguchi H, Nakadomari S, Misaki M, Wandell BA. Two temporal channels in human V1 identified using fMRI. Neuroimage. 2009; 47:273–280. [PubMed: 19361561]

Ichida JM, Schwabe L, Bressloff PC, Angelucci A. Response facilitation from the "suppressive" receptive field surround of macaque V1 neurons. J Neurophysiol. 2007; 98:2168–2181. [PubMed: 17686908]

Itti L, Koch C, Braun J. Revisiting spatial vision: toward a unifying model. J Opt Soc Am A Opt Image Sci Vis. 2000; 17:1899–1917. [PubMed: 11059585]

Kastner S, Pinsk MA, De Weerd P, Desimone R, Ungerleider LG. Increased activity in human visual cortex during directed attention in the absence of visual stimulation. Neuron. 1999; 22:751–761. [PubMed: 10230795]

Kayama Y, Riso RR, Bartlett JR, Doty RW. Luxotonic responses of units in macaque striate cortex. J Neurophysiol. 1979; 42:1495–1517. [PubMed: 115968]

Kleinschmidt A, Lee BB, Requardt M, Frahm J. Functional mapping of color processing by magnetic resonance imaging of responses to selective P- and M-pathway stimulation. Exp Brain Res. 1996; 110:279–288. [PubMed: 8836691]

Kruger J. The shift-effect in the lateral geniculate body of the rhesus monkey. Exp Brain Res. 1977; 29:387–392. [PubMed: 410653]

Lee BB, Sun H. The chromatic input to cells of the magnocellular pathway of primates. J Vis. 2009; 9(15):11–18.

Li X, Lu ZL, Tjan BS, Dosher BA, Chu W. Blood oxygenation level-dependent contrast response functions identify mechanisms of covert attention in early visual areas. Proc Natl Acad Sci U S A. 2008; 105:6202–6207. [PubMed: 18413602]

Ling S, Liu T, Carrasco M. How spatial and feature-based attention affect the gain and tuning of population responses. Vision Res. 2008

Liu J, Wandell BA. Specializations for chromatic and temporal signals in human visual cortex. J Neurosci. 2005; 25:3459–3468. [PubMed: 15800201]

Logothetis NK, Wandell BA. Interpreting the BOLD signal. Annu Rev Physiol. 2004; 66:735–769. [PubMed: 14977420]

Logothetis NK, Murayama Y, Augath M, Steffen T, Werner J, Oeltermann A. How not to study spontaneous activity. Neuroimage. 2009; 45:1080–1089. [PubMed: 19344685]

MacLeod DI, Boynton RM. Chromaticity diagram showing cone excitation by stimuli of equal luminance. J Opt Soc Am. 1979; 69:1183–1186. [PubMed: 490231]

McKee SP, Taylor DG. Discrimination of time: comparison of foveal and peripheral sensitivity. J Opt Soc Am A. 1984; 1:620–627. [PubMed: 6336556]

Movshon JA, Thompson ID, Tolhurst DJ. Spatial summation in the receptive fields of simple cells in the cat's striate cortex. J Physiol. 1978; 283:53–77. [PubMed: 722589]

Palmer LA, Davis TL. Receptive-field structure in cat striate cortex. J Neurophysiol. 1981; 46:260–276. [PubMed: 6267213]

Petrov Y, McKee SP. The time course of contrast masking reveals two distinct mechanisms of human surround suppression. J Vis. 2009; 9(21) 21-11.

Petrov Y, Carandini M, McKee S. Two distinct mechanisms of suppression in human vision. J Neurosci. 2005; 25:8704–8707. [PubMed: 16177039]

Petrov Y, Popple AV, McKee SP. Crowding and surround suppression: not to be confused. J Vis. 2007; 7(12):11–19.

Priebe NJ, Ferster D. Inhibition, spike threshold, and stimulus selectivity in primary visual cortex. Neuron. 2008; 57:482–497. [PubMed: 18304479]

Priebe NJ, Mechler F, Carandini M, Ferster D. The contribution of spike threshold to the dichotomy of cortical simple and complex cells. Nat Neurosci. 2004; 7:1113–1122. [PubMed: 15338009]

Ress D, Backus BT, Heeger DJ. Activity in primary visual cortex predicts performance in a visual detection task. Nat Neurosci. 2000; 3:940–945. [PubMed: 10966626]

Reynolds JH, Heeger DJ. The normalization model of attention. Neuron. 2009; 61:168–185. [PubMed: 19186161]

Sayres R, Grill-Spector K. Object-selective cortex exhibits performance-independent repetition suppression. J Neurophysiol. 2006; 95:995–1007. [PubMed: 16236787]

Schira MM, Wade AR, Tyler CW. Two-dimensional mapping of the central and parafoveal visual field to human visual cortex. J Neurophysiol. 2007; 97:4284–4295. [PubMed: 17360817]

Schira MM, Fahle M, Donner TH, Kraft A, Brandt SA. Differential contribution of early visual areas to the perceptual process of contour processing. J Neurophysiol. 2004; 91:1716–1721. [PubMed: 14668291]

Sereno MI, Dale AM, Reppas JB, Kwong KK, Belliveau JW, Brady TJ, Rosen BR, Tootell RB. Borders of multiple visual areas in humans revealed by functional magnetic resonance imaging. Science. 1995a; 268:889–893. [PubMed: 7754376]

Sereno MI, Dale AM, Reppas JB, Kwong KK, Belliveau JW, Brady TJ, Rosen BR, Tootell RB. Borders of multiple human visual areas in humans revealed by functional mri. Science. 1995b; 268:889–893. [PubMed: 7754376]

Shadlen MN, Britten KH, Newsome WT, Movshon JA. A computational analysis of the relationship between neuronal and behavioral responses to visual motion. J Neurosci. 1996; 16:1486–1510. [PubMed: 8778300]

Shmuel A, Augath M, Oeltermann A, Logothetis NK. Negative functional MRI response correlates with decreases in neuronal activity in monkey visual area V1. Nat Neurosci. 2006; 9:569–577. [PubMed: 16547508]

Shmuel A, Yacoub E, Pfeuffer J, Van de Moortele PF, Adriany G, Hu X, Ugurbil K. Sustained negative BOLD, blood flow and oxygen consumption response and its coupling to the positive response in the human brain. Neuron. 2002; 36:1195–1210. [PubMed: 12495632]

Sirotin YB, Das A. Anticipatory haemodynamic signals in sensory cortex not predicted by local neuronal activity. Nature. 2009; 457:475–479. [PubMed: 19158795]

Smith AT, Williams AL, Singh KD. Negative BOLD in the visual cortex: evidence against blood stealing. Hum Brain Mapp. 2004; 21:213–220. [PubMed: 15038003]

Smith MA, Bair W, Movshon JA. Dynamics of suppression in macaque primary visual cortex. J Neurosci. 2006; 26:4826–4834. [PubMed: 16672656]

Solomon SG, White AJ, Martin PR. Extraclassical receptive field properties of parvocellular, magnocellular, and koniocellular cells in the primate lateral geniculate nucleus. J Neurosci. 2002; 22:338–349. [PubMed: 11756517]

Solomon SG, Peirce JW, Lennie P. The impact of suppressive surrounds on chromatic properties of cortical neurons. J Neurosci. 2004; 24:148–160. [PubMed: 14715948]

Solomon SG, Lee BB, Sun H. Suppressive surrounds and contrast gain in magnocellular-pathway retinal ganglion cells of macaque. J Neurosci. 2006; 26:8715–8726. [PubMed: 16928860]

Stockman A, MacLeod DI, Johnson NE. Spectral sensitivities of the human cones. J Opt Soc Am A Opt Image Sci Vis. 1993; 10:2491–2521. [PubMed: 8301403]

Teo PC, Sapiro G, Wandell BA. Creating connected representations of cortical gray matter for functional MRI visualization. IEEE Trans Med Imaging. 1997; 16:852–863. [PubMed: 9533585]

Tootell RB, Mendola JD, Hadjikhani NK, Liu AK, Dale AM. The representation of the ipsilateral visual field in human cerebral cortex. Proc Natl Acad Sci U S A. 1998a; 95:818–824. [PubMed: 9448246]

Tootell RB, Hadjikhani N, Hall EK, Marrett S, Vanduffel W, Vaughan JT, Dale AM. The retinotopy of visual spatial attention. Neuron. 1998b; 21:1409–1422. [PubMed: 9883733]

Treue S, Martinez Trujillo JC. Feature-based attention influences motion processing gain in macaque visual cortex. Nature. 1999; 399:575–579. [PubMed: 10376597]

Tyler CW, Hamer RD. Analysis of visual modulation sensitivity. IV. Validity of the Ferry-Porter law. J Opt Soc Am A. 1990; 7:743–758. [PubMed: 2338596]

Tyler CW, Hamer RD. Eccentricity and the Ferry-Porter law. J Opt Soc Am A Opt Image Sci Vis. 1993; 10:2084–2087. [PubMed: 8410438]

Wade A, Wandell B. Cone Specific Color Adaptation Measured in Human V1. 2002

Wandell BA, Poirson AB, Newsome WT, Baseler HA, Boynton GM, Huk A, Gandhi S, Sharpe LT. Color signals in human motion-selective cortex. Neuron. 1999; 24:901–909. [PubMed: 10624953]

Watson AB, Pelli DG. QUEST: a Bayesian adaptive psychometric method. Percept Psychophys. 1983; 33:113–120. [PubMed: 6844102]

Webb BS, Dhruv NT, Solomon SG, Tailby C, Lennie P. Early and late mechanisms of surround suppression in striate cortex of macaque. J Neurosci. 2005; 25:11666–11675. [PubMed: 16354925]

Williams PE, Mechler F, Gordon J, Shapley R, Hawken MJ. Entrainment to video displays in primary visual cortex of macaque and humans. J Neurosci. 2004; 24:8278–8288. [PubMed: 15385611]

Williford T, Maunsell JH. Effects of spatial attention on contrast response functions in macaque area V4. J Neurophysiol. 2006; 96:40–54. [PubMed: 16772516]

Xing J, Heeger DJ. Center-surround interactions in foveal and peripheral vision. Vision Res. 2000; 40:3065–3072. [PubMed: 10996610]

Xing J, Heeger DJ. Measurement and modeling of center-surround suppression and enhancement. Vision Res. 2001; 41:571–583. [PubMed: 11226503]

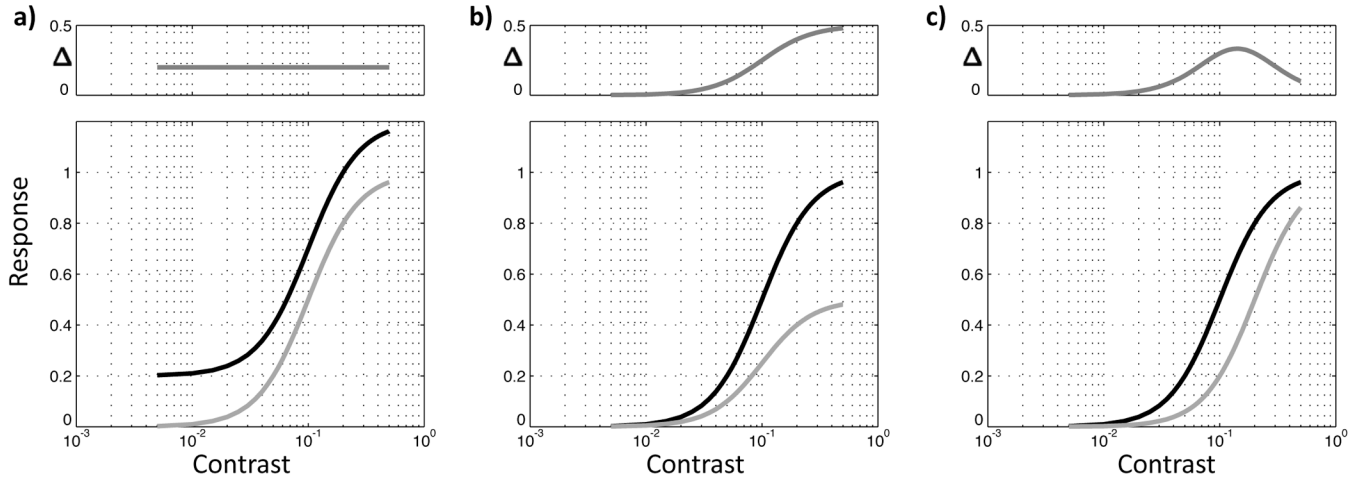

Figure 1.

Candidate models of NBR-related neural suppression. Black curves represent neural responses without suppression, and light grey curves represent neural responses after suppression under the assumptions of each model. The differences (Δ) between the suppressed and unsuppressed curves are shown in the small plots above each model. a) The subtractive mechanism model predicts that the difference is independent of contrast. b) The response gain model predicts that the difference grows with increasing contrast. c) The contrast gain model predicts that the difference is non-monotonic, depending upon the form of the contrast response function and approaching zero at high contrast. Contrast scale is 0–1, responses are in arbitrary units.

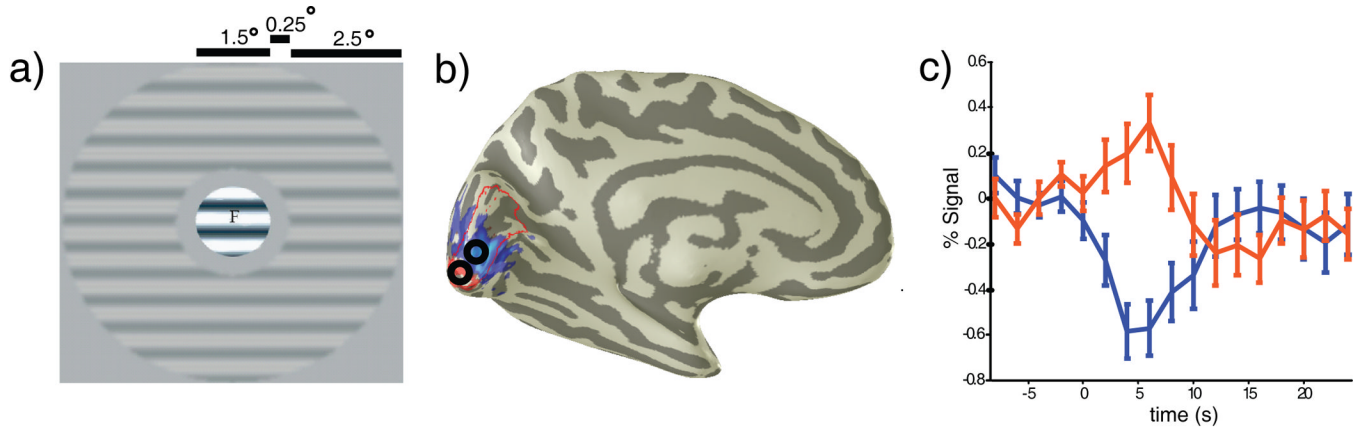

Figure 2.

Example of stimulus configuration and typical responses. a) Stimuli used in the fMRI scans, showing both the central inducer, and the surround region with contrast-reversing sine-wave gratings. The central region could be set to either 90% or 0% contrast, and the surround region was set to C_s levels of either 0%, 5%, 20%, or 45% contrast. 'F' marks the location of the foveal letter discrimination task. b) Map showing typical response amplitudes to a high-resolution central region with 0% surround contrast rendered on a single inflated hemisphere. The location of area V1 is outlined in red. Positive responses are rendered in red and are found at the occipital pole. Some responses are not visible as they extend onto the lateral surface. A large swath of visual cortex also demonstrates a negative BOLD response (blue) extending well into the periphery. c) Response timecourses measured from disks over peripheral (blue) and foveal (red) locations in panel b).

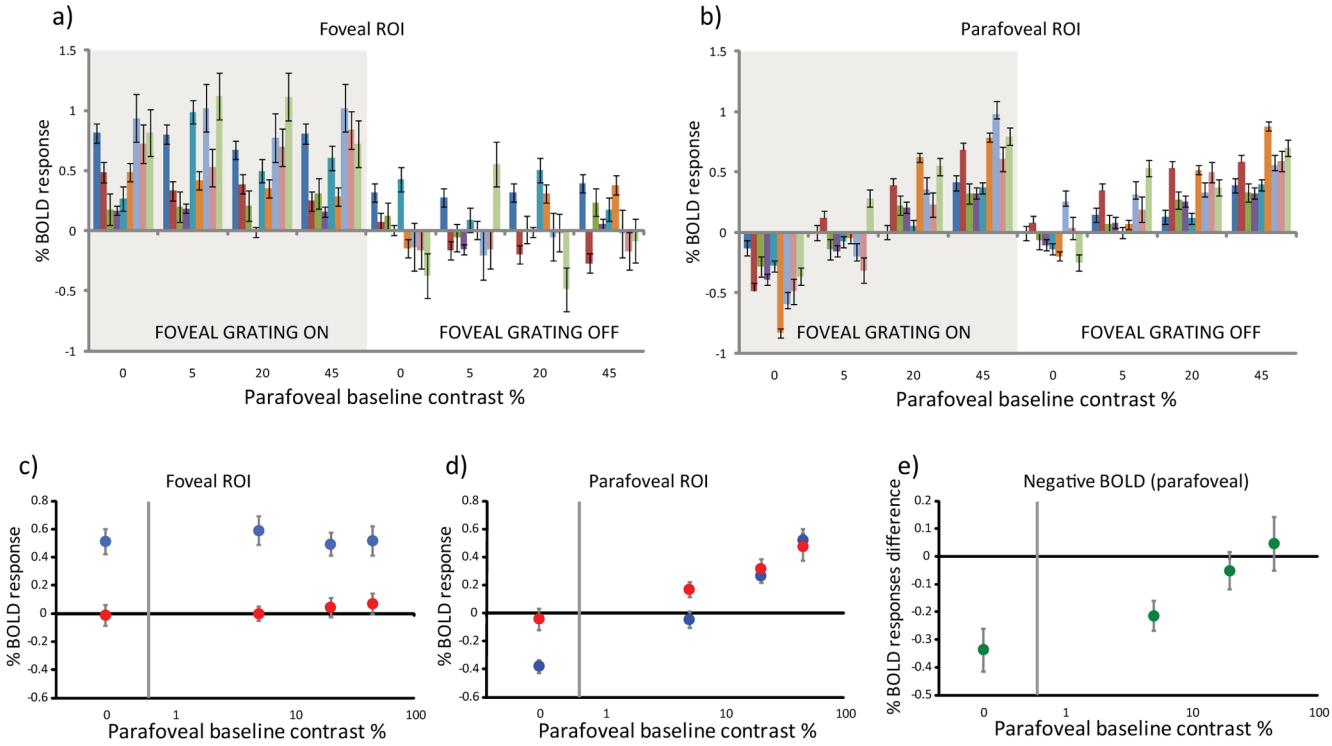

Figure 3.

Raw BOLD responses in the fovea (3a) and surround (3b). The response amplitudes for each level of surround contrast are plotted for both conditions with and without the presence of the central high-contrast inducer. The different colored bars represent BOLD amplitudes for each individual subject. Error bars are between-trial SEMs. Average data for the foveal and parafoveal ROIs are shown in 3c and 3d respectively. Blue data points represent conditions without the inducer (0% center contrast), and red data points represent conditions with the inducer (90% center contrast). Data points in 3e represent the difference in surround BOLD response between identical surround contrast conditions with and without the presence of the inducer. Error bars are 1SEM computed across subjects.

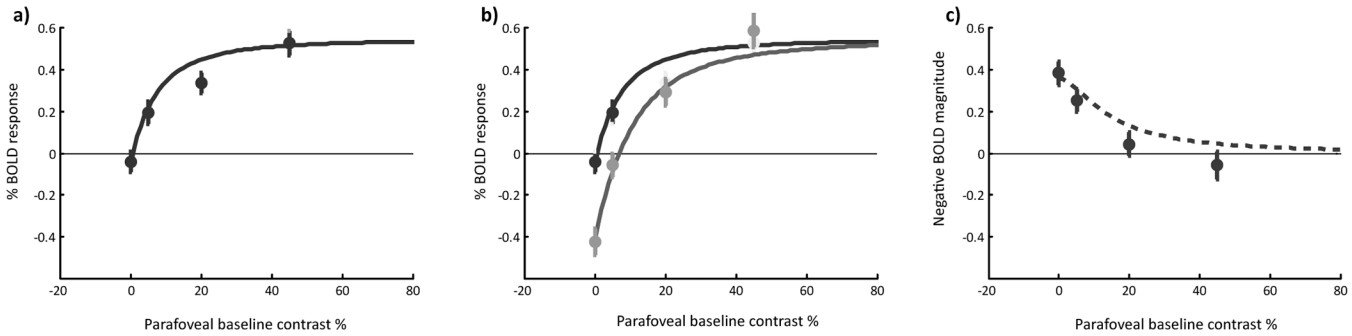

Figure 4.

a,b) Fits of a hyperbolic ratio function to contrast responses measured in the probe region. Unsuppressed data shown in black, suppressed data shown in gray. The same function is used to fit both curves – the only difference being a multiplicative (x 0.62) scaling on the input contrast in the presence of a central inducer. c) Negative BOLD amplitudes in the probe region with modeled NBR curve overlaid. The model captures both qualitative and quantitative features of the data. Fitted parameters: k=1.71, σ=6.8%, C_0=9.36%, A=−1.14.

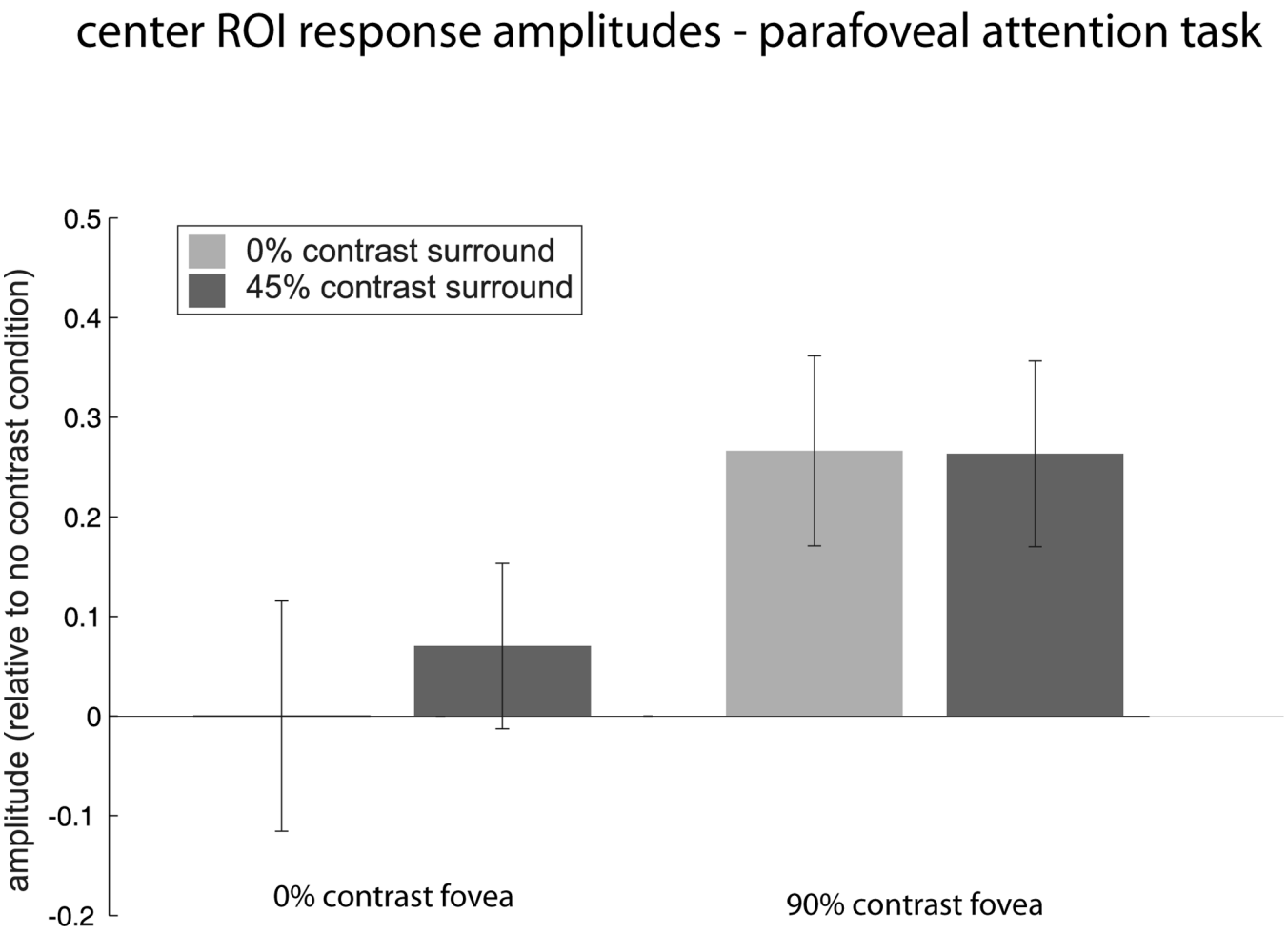

Figure 5.
Center ROI response amplitudes, averaged for three subjects, with both no contrast and with 90% high contrast center. All measurements were taken while subjects performed a demanding parafoveal attention task. For both levels of central contrast, the addition of a 45% contrast surround (dark bars) produces no effect of suppression, consistent with results from the same experiment with a foveal attention task. This suggests that attentional demands do not drive the results we see for the central region.

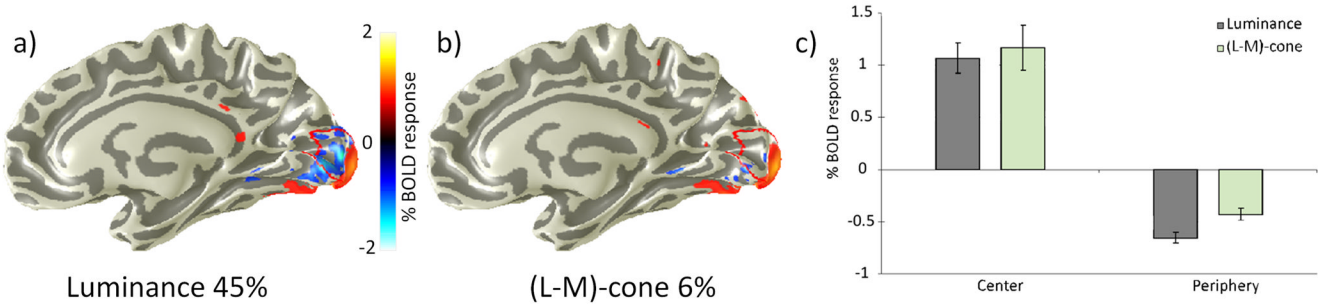

Figure 6.

Isoluminant stimuli generate a weaker NBR. Renderings of BOLD response amplitudes from a single subject's right hemisphere showing responses to high-contrast, foveal a) luminance and b) opponent (L−M)-cone stimuli. Both stimulus types generate a strong positive response in the foveal region of area V1 (outlined in red). Only the luminance contrast also generates a strong NBR (coded as blue). c) Average amplitudes of positive and negative BOLD response averaged across four subjects. Mean cone contrasts were chosen to generate approximately equal responses in the directly-stimulated locations. Error bars are 1SEM. See also Supplementary Figure S2.

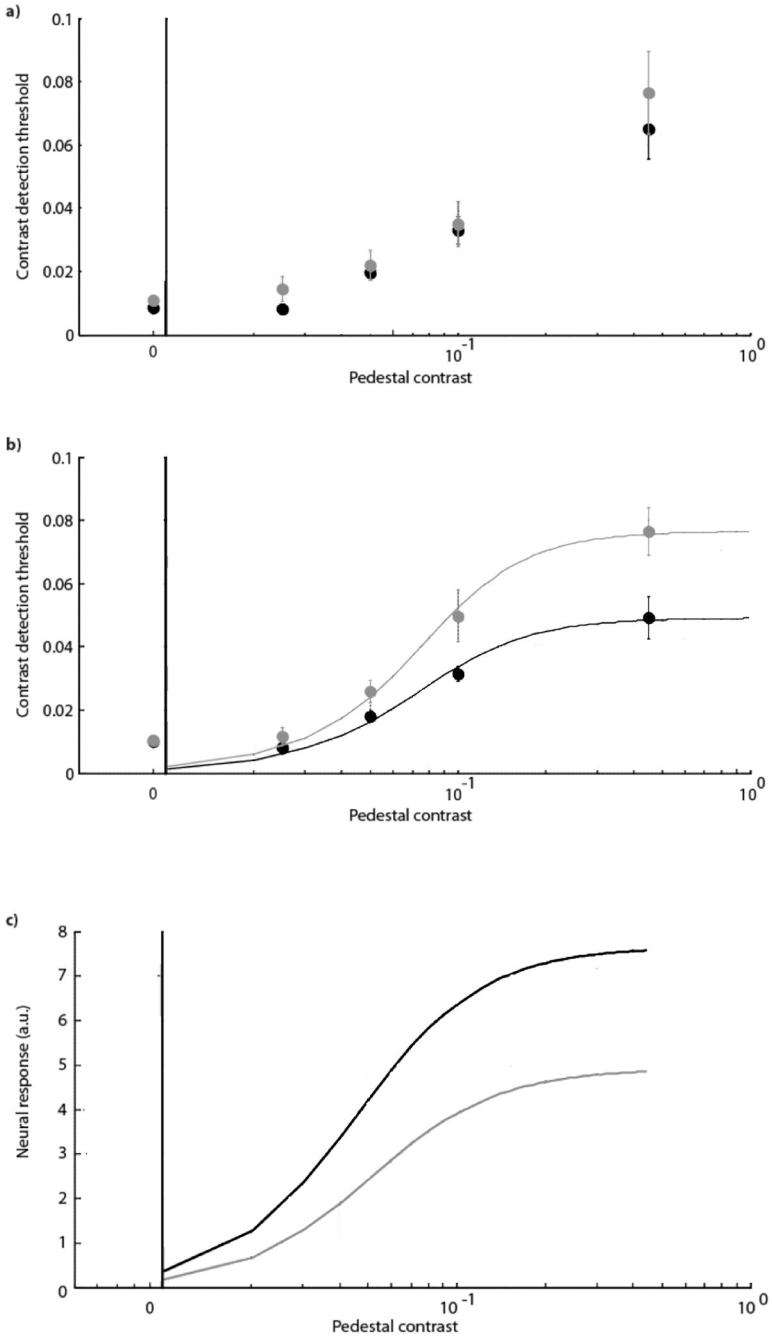

Figure 7.

a,b) Average threshold-versus-contrast data for five subjects. Thresholds measured in the presence of a mask are shown in gray, thresholds measured in isolation are shown in black. Contrast scale is 0–1. a) Foveal target b) Parafoveal target. The foveal target shows no statistically-significant evidence of suppression due to the remote, high contrast annulus. In comparison, thresholds in the parafoveal, annular target are elevated significantly by the high-contrast foveal disk. The fits in panel b) were made by assuming that thresholds are determined by the Fischer information of the neural responses at each contrast level with the underlying neural response function being given by a hyperbolic ratio function of the form shown in Equation 1. c) Estimated neural contrast response functions for unsuppressed

(black) and suppressed (gray) parafoveal target conditions based on psychophysical contrast discrimination thresholds. The fitted parameters in both b) and c) are the same: k (response gain) and σ (semi-saturation constant). Suppressed: k=8, σ=0.05; Unsuppressed: k=5, σ=0.05). The primary effect of suppression is to change the parameter k, consistent with a response gain mechanism.